



Investigation of the compatibility between kaempferol and excipients by thermal, spectroscopic and chemometric methods

Gabriela de Lima Melchiades¹ · Valéria Weiss Angeli² · Mariana Colombo¹ · Letícia Scherer Koester¹

Received: 28 May 2019 / Accepted: 23 November 2019 / Published online: 12 December 2019
© Akadémiai Kiadó, Budapest, Hungary 2019

Abstract

Compatibility is an important step in pre-formulation studies during the development of solid dosage forms. In the present study, we used thermal analysis (differential scanning calorimetry and thermogravimetry), isothermal stress testing followed by high-performance liquid chromatography and Fourier transform infrared spectroscopy complemented by two multivariate techniques (hierarchical cluster analysis and principal component analysis) to detect potential incompatibilities between kaempferol and commonly used solid dosage form excipients in binary mixtures. The excipients that were studied were starch, microcrystalline cellulose, magnesium stearate, hydroxypropylmethylcellulose, lactose, sodium lauryl sulfate and polyvinylpyrrolidone. The thermal analyses results indicated interactions occurred between kaempferol and all excipients studied except microcrystalline cellulose. However, infrared spectroscopy complemented by multivariate analysis indicated compatibility between kaempferol and all excipients. Isothermal stress testing confirmed the absence of significant change in the content of kaempferol in the binary mixtures. Our study demonstrates the importance of combining different techniques and multivariate data analysis for pre-formulation drug-excipient analysis.

Keywords Kaempferol · Excipients · Compatibility · Thermal analysis · Cluster analysis · Principal component analysis

Introduction

The quality of a pharmaceutical formulation depends not only on the choice of active substance and the production process, but also on the appropriate selection of excipients [1–3]. In the pre-formulation stage of development, the study of drug-excipient compatibility is one of the most important steps as it enhances the understanding of drug-excipient interactions and highlights changes in the physical or chemical properties of the drug and/or therapeutic response [3–5]. Compatibility screening involves the analysis of mixtures of the drug with one or more excipients.

Thermoanalytical techniques such as differential scanning calorimetry (DSC) and thermogravimetry (TG) are used for a quick screening due to their ease of use [6, 7]. Although spectroscopic techniques such as Fourier transform infrared spectroscopy (FTIR) are also easily conducted, the volumes of data that are generated limit their use as interpretation is labor intensive. Quantitative assay after isothermal stress test (IST) is another tool that is used to detect drug-excipient interactions [5, 7, 8].

Chemometrics is currently employed to assist the complex interpretation of a large variety of data, and uses common mathematical and statistical methods to maximize the information that is extracted from chemical data [9]. Chemometrics can be used to support many techniques, including infrared spectroscopy [10]. Principal component analysis (PCA) is a method of multivariate data treatment that reduces the dimensionality of data while maintaining the variation present in the data group [7, 11]. On the other hand, hierarchical cluster analysis (HCA) measures the similarity between samples and classifies them into groups with similar spectral characteristics using the Euclidean distance [12–14].

✉ Letícia Scherer Koester
leticia.koester@ufrgs.br

¹ Laboratório de Desenvolvimento Galênico, Programa de Pós-Graduação em Ciências Farmacêuticas, Faculdade de Farmácia, Universidade Federal do Rio Grande do Sul, Av. Ipiranga, 2752/607, Porto Alegre, RS 90.610-000, Brazil

² Programa de Pós-Graduação em Engenharia de Processos e Tecnologias, Universidade de Caxias do Sul - Campus-Sede, Caxias do Sul, RS, Brazil

Flavonoids are polyphenolic compounds synthesized naturally by plants and widely distributed in the plant kingdom and contained in common human diet [15, 16]. Kaempferol (KPF, 3,5,7-trihydroxy-2-(4-hydroxyphenyl)-4H-1-benzopyran-4-one, Fig. 1) [17], is a flavonoid with a wide range of pharmacological properties including anti-inflammatory, antibacterial, antiviral, antifungal, antiapoptotic and antioxidant properties [18, 19]. However, the clinical application of KPF is limited by its poor water solubility and low bioavailability after oral administration [16, 20]. Strategies to increase the solubility and bioavailability of KPF *in vitro* and *in vivo* have been developed [16, 19–25]. Due to the wide range of pharmacological properties the kaempferol is an attractive ingredient for the development of solid dosage forms, meaning that this flavonoid can be classified as a drug candidate. However, prior to the development of new pharmaceutical forms, drug–excipient compatibility studies must be carried out.

The aim of this study was, therefore, to evaluate the compatibility of KPF with selected excipients commonly used in the development of solid dosage forms. The excipients studied were starch, microcrystalline cellulose, magnesium stearate, hydroxypropylmethylcellulose, lactose, sodium lauryl sulfate and polyvinylpyrrolidone; and the mixtures were assessed using thermal analysis (DSC and TG), IST and spectroscopic techniques (FTIR), the last combined with PCA and HCA. To our knowledge, this is the first time that such studies have been carried out on KPF.

Experimental

Materials

Stocks of KPF (98.18% purity) were purchased from ShaanXi HuiKe Botanical (Xi'an, China). The pharmaceutical excipients were purchased from different

manufacturers: corn starch (STR) from Corn Products (São Paulo, Brazil), microcrystalline cellulose 101 (MCC) from Minitai Chemical CO., LTD (Taiwan, China), magnesium stearate (MS) from Forlab (Rio de Janeiro, Brazil), hydroxypropylmethylcellulose (HPMC, methocel K100) from Colorcon (PA, USA), lactose monohydrate M-200 (LAC) from Milkaut (Pcia. de Santa Fé, Argentina), sodium lauryl sulfate (SLS) from CQA (São Paulo, Brazil), polyvinylpyrrolidone (PVP) from Vetec (Rio de Janeiro, Brazil). Formic Acid 96% and Methanol HPLC grade (used for the preparation of the mobile phase) were obtained from Tedia (Rio de Janeiro, Brazil). Ultrapure water was produced with a Milli-Q system (Millipore, Billerica, USA). All other used reagents were of analytical grade.

Methods

Preparation of KPF–excipient binary mixtures

Mixtures of KPF with each of the seven excipients were prepared in 1:1 ratios (w/w KPF/excipient) in glass vials, then homogenized by vortexing for 3 min.

Differential scanning calorimetry

The DSC curves of KPF, excipients and binary mixtures were obtained using a Shimadzu Calorimeter Model DSC-60A (Kyoto, Japan) calibrated with an indium standard (156.6 ± 0.3 °C). The samples were weighed directly in aluminum pans (the mass of samples that were used were 1–2 mg), sealed and scanned under a dry atmosphere of nitrogen (50 mL min^{-1}) with a heating flow rate of 10 °C min^{-1} in the temperature range of 10–400 °C.

Thermogravimetric analysis

Thermogravimetric analysis of KPF alone and the binary mixtures was carried out using a Shimadzu Thermogravimetric Model TGA-50 (Kyoto, Japan) under a nitrogen atmosphere (50 mL min^{-1}) with a heating flow rate of 10 °C min^{-1} in the temperature range 23–800 °C. The mass of samples that were used were approximately 10 mg.

Fourier transform infrared spectroscopy

The FTIR spectra of KPF, the excipients and the binary mixtures were obtained using a spectrophotometer (PerkinElmer, Model BX/RX, Connecticut, USA) in the range 4000 – 600 cm^{-1} , with a resolution of 2 cm^{-1} over 40 scans.

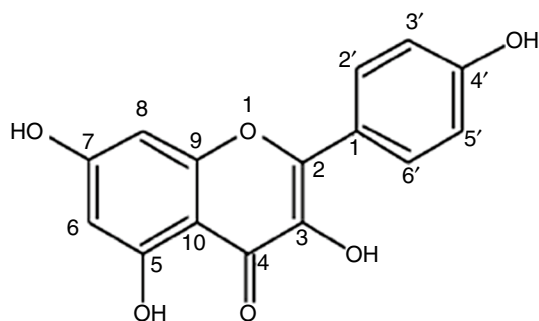
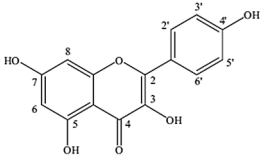
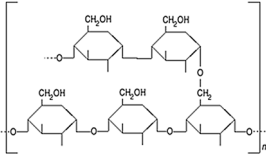
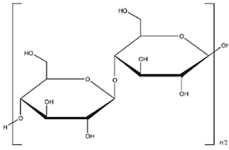
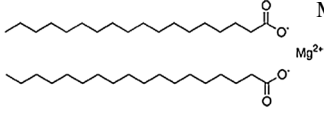
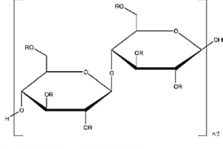
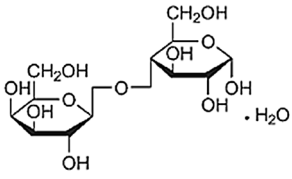
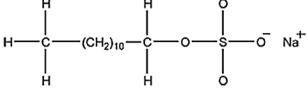
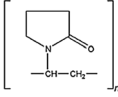


Fig. 1 Chemical structure of Kaempferol

Table 1 General characterization of kaempferol and the excipients used

Samples	M.F. M.M.	Chemical structure	Heat changes of kaempferol and excipients	
			DSC data	References
Kaempferol	$C_{15}H_{10}O_6$ 286.24		Melt peak, 287.89 °C	Melt peak, 285.5 °C [15];
STR	$(C_6H_{10}O_5)_n$ (164.12) _n		Dehydration, 65.89 °C Decomposition, 299.08 °C	Dehydration, 72 °C Decomposition, 285; 315 °C [3]
MCC	$(C_6H_{10}O_5)_n$; $n \approx 220$ (162.141) _n		Dehydration, 50.28 °C Decomposition, 353.98 °C	Dehydration, 50 °C Decomposition, 315 °C [6] Dehydration, 53 °C Decomposition, 332; 357 °C [3]
MS	$(C_{18}H_{35}O_2)_2Mg$ 591.24		Melt peak, 110.85 °C	Melt peak, 115 °C [3]
HPMC	$C_{12}H_{20}O_{11}R_6$ R=H or, CH ₃ or, CH ₃ CH(OH)CH ₂ 10.000-1.500.00	 <small>where R is H, CH₃, or CH₃CH(OH)CH₂</small>	Dehydration, 56.88 °C Decomposition, 337.99 °C	Dehydration, 66.22 °C [2]
LAC	$C_{12}H_{22}O_{11} \cdot H_2O$ 360.31	 α -Lactose monohydrate	Dehydration, 147.22 °C Melt peak, 217.85 °C Decomposition, 242.34; 355.20 °C	Dehydration, 152.7 °C Melt peak, 218.38 °C [8] Dehydration, 145.00 °C Melt peak, 215.00 °C [6]
SLS	$C_{12}H_{25}NaO_4S$ 288.38		Dehydration, 104.42 °C Melt peak, 190.15 °C Decomposition, 271.34 °C	Dehydration, 95; 107 °C Melt peak, 192 °C Decomposition, 223 °C [3]
PVP	$(C_6H_9NO)_n$ (111.14) _n		Melt peak, 73.20 °C Decomposition, 376.52 °C	Melt peak, 82 °C [6]

M.F. Molecular formula

M.M. Molar mass

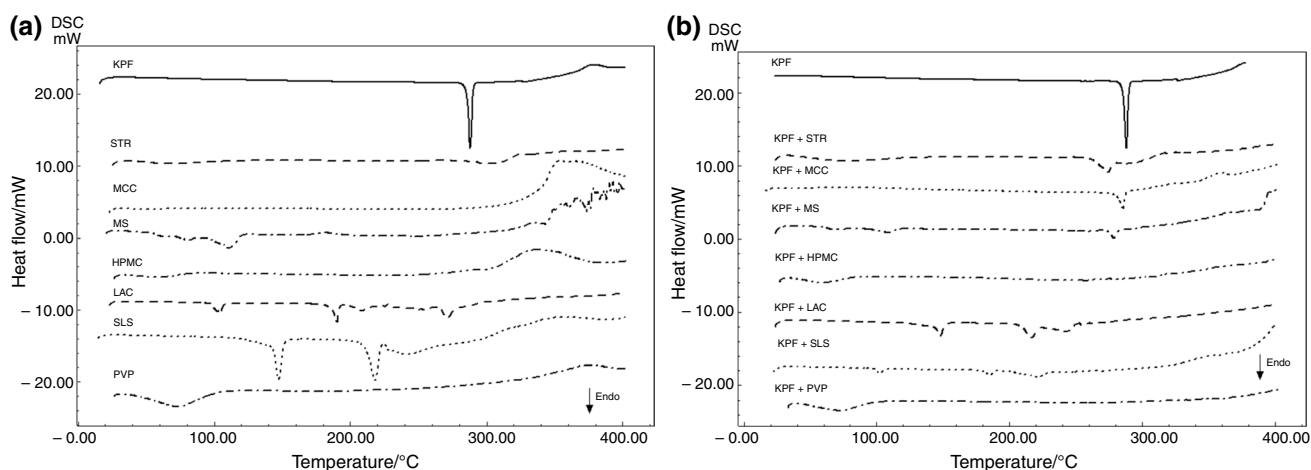


Fig. 2 a DSC curves of KPF and the excipients alone; b DSC curves of KPF and binary mixtures at 10–400 °C; heating rate 10 °C min⁻¹; atmosphere of nitrogen, 50 mL min⁻¹

Multivariate analysis

The PCA and HCA analyses were performed using SPSS Statistics 22[®] software (IBM Corp. Released 2013) [26]. From the FTIR spectra of the samples, a data matrix with a size of 15 × 2000 was obtained, where 15 is the number of columns (KPF, excipients and their binary mixtures) and 2000 is the number of lines (absorbance values of samples). All data acquired from the FTIR spectra were normalized between the limits of zero and one, corrected using the multiple scatter correction method (MSC) and Savitzky–Golay method from data centered on the mean [7, 12].

Isothermal stress testing

The drug and excipient samples were weighed directly in glass vials ($n = 3$) and mixed using a vortex for 3 min. Stressed samples were produced by adding water (10% w/w), sealing each vial using a Teflon-lined screw cap and storing in a hot air oven at 50 °C. After 3 weeks, the samples were diluted appropriately to 5 µg ml⁻¹ then quantitatively analyzed using HPLC and qualitatively through assessment of color change. The KPF–excipient mixtures were stored undiluted in a refrigerator at 4 °C to serve as controls (control samples) [1, 6]. Analysis of the KPF–excipient mixtures was performed on an HPLC apparatus (Shimadzu LC-10A system, Kyoto,

Japan) equipped with a model LC-20AT pump, an SPD-20AV UV–VIS variable wavelength detector, a DGU-20A5 degasser, a CBM-20A system controller and SIL-20A injection valve with a 100 µL loop. The KPF sample was analyzed using a XTerra[®] RP18 column (250 mm × 4.6 mm, 5 µm particle size) (Waters, Milford, MA, USA). The mobile phase was a 75:25 (v/v) mixture of methanol and 0.1% formic acid in water. The injection volume was 20 µL, and the HPLC system was operated at an isocratic flow rate of 1.0 mL min⁻¹, with detection at 368 nm and temperature of 35 °C [27].

Results and discussion

Thermal analyses

Basic information about the thermal profiles of KPF and the excipients is given in Table 1. The thermal profile of pure KPF presented a single-step melting process with no dehydration step (Fig. 2). The DSC curve showed a sharp endothermic peak at 287.89 °C, indicating the melting point of KPF, which is in agreement with the literature [15]. In the TG curve, mass losses relating to KPF decomposition were observed in three events: 32.15% at 318–324 °C, 39.30% at 450–550 °C and 31.60% at 780 °C (Fig. 3). Both MS and SLS melted at 100–200 °C; LAC melted above 200 °C and STR, MCC, HPMC and

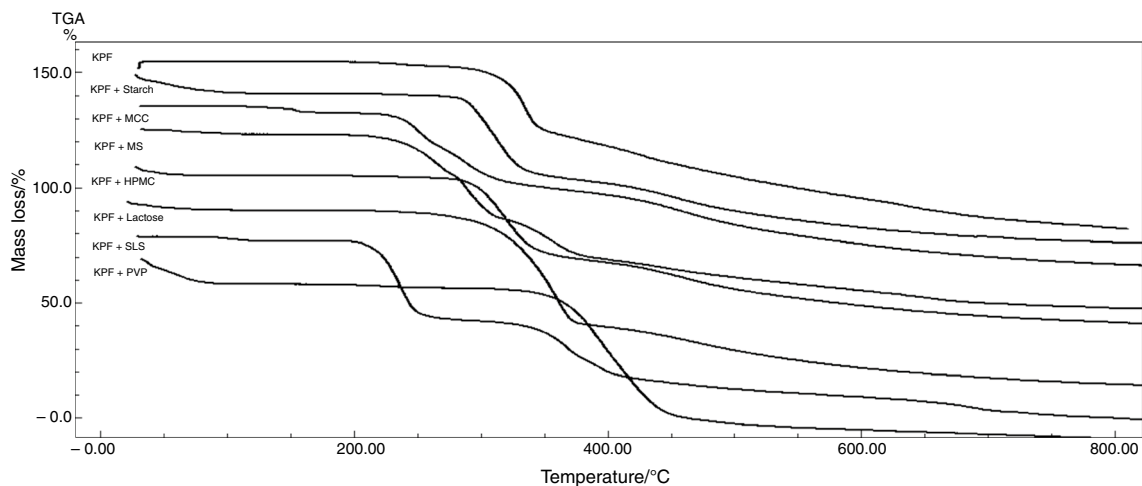


Fig. 3 TG curves of KPF and binary mixtures at 10–800 °C, heating rate 10 °C min⁻¹; atmosphere of nitrogen, 50 mL min⁻¹

PVP began to decompose above 200 °C which led to charring.

The heat effects associated with physical or chemical changes of a sample can be observed with DSC. The appearance or disappearance of one or more peaks and changes in melting temperature when a substance is analyzed as part of a mixture are considered indicative of interactions between components [8, 10].

The DSC curves obtained in this study revealed KPF to have an endothermic melting peak of 285.29 °C in the KPF–MCC mixture. This is not significantly different to the melting point of KPF alone, which suggests that there was no interaction between MCC and KPF. However, DSC analysis of all other mixtures indicated that KPF–excipient interactions were occurring. In the case of STR and MS, the endothermic peak was shifted and the peak size was reduced. The HPMC–, LAC–, SLS– and PVP–KPF curves showed no endothermic melting peak of KPF, which suggests interaction between them (Fig. 2 and Table 2).

Variations in the shape of TG curves may be considered to indicate drug–excipient interactions, but the changes are not usually as dramatic as those observed by DSC. Because TG curves reveal mass losses which accompany phase transitions (for example, sublimation and evaporation) that occur in analyzed mixtures, it was not possible to confirm whether ingredients of the mixtures were compatible (Table 2). Thus, it is verified that this technique must be evaluated in conjunction with other thermal analysis techniques (Fig. 3) [10].

The results of DSC and TG analyses indicated that KPF–excipient interactions were occurring in the case of

STR, MS, HPMC, LAC, SLS and PVP. However, these results may be attributed to the high temperatures used during the experiment. In these conditions, the excipients may melt and influence the solubility of KPF, which can interfere with the reading [2]. Due to the potential limitations of thermal techniques, complementary methods of analysis were carried out to aid the interpretation of data and acquire as much information as possible.

Fourier transform infrared analysis

Among the spectroscopic methods, FTIR has the advantages of requiring only a small amount of sample and being less destructive than other methods. It is therefore an attractive approach for the analysis of solid dosage forms, since the materials are not subjected to thermal or mechanical energies during preparation and solid-state phase transformations avoided [3]. Drug–excipient interactions can usually be identified by the appearance of new absorption bands and the broadening and/or alteration of band intensities compared with individual component spectra [7, 8]. The FTIR spectrum of KPF is shown in Fig. 4, the characteristic bands were as follows: (1) a strong and wide band at 3319 cm⁻¹ attributed to the four hydroxyls (stretching vibration of O–H); (2) a 1654 cm⁻¹ displaced carbonyl band due to the inductive effect of the resonance of α - and β -unsaturated ketones (C=O); (3) a band at 1616 cm⁻¹ indicating aromatic compounds (C=C); (4) a band at 1508 cm⁻¹ due to benzene ring vibrations; (5) a

Table 2 Thermoanalytical data of KPF and their binary mixtures 1:1 with kaempferol

Samples	Dehydration			Fusion			Decomposition			
	DSC		TG	DSC		TG	DSC		TG	
	$T_{\text{peak}}/^{\circ}\text{C}$	$\Delta H_{\text{corr}}/\text{J g}^{-1}$	$\Delta m/\%$	$T_{\text{onset (fusion)}/^{\circ}\text{C}}$	$\Delta H_{\text{corr}}/\text{J g}^{-1}$	$T_{\text{peak}}/^{\circ}\text{C}$	$\Delta H_{\text{corr}}/\text{J g}^{-1}$	$T_{\text{peak}}/^{\circ}\text{C}$	$\Delta T/^{\circ}\text{C}^{\text{a}}$	$\Delta m/\%$
KPF	–	–	32.15	285.70	–134.69	287.89	–151.69	370	318–324	32.15
KPF + STR	76.72	–276.22	5.95	273.31	–86.64	274.38	111.1	301.32	450–550;	39.30;
KPF + MCC	40.48	–12.40	2.32	281.69	–101.82	285.29	29.74	339.48	290–329;	36.26;
KPF + MS	69.25	–47.43	1.97;	274.83	–64.71	278.52	57.92	391.09	420–558	28.29
	259.64	–26.85	15.59				–8.61	285.21	324–371;	51.40;
KPF + HPMC	59.05	–202.47	1.93	–	–	–	–198.62	392.87	381–576	24.85
							–93.18	320.48	284–301;	22.79;
KPF + LAC	147.70	–176.54	2.81	–	–	–	–104.47	240.60	340–387	25.66
							–		293–338;	35.44;
KPF + SLS	102.24	–33.94	1.91	–	–	–	–	221.12	458–549	30.07
							–		236–286;	32.16;
KPF + PVP	72.70	–381.98	7.83	–	–	–	–	375.22	439–487	22.00
							–		220–248;	34.48;
							–		347–394;	29.38;
							–		643–713	12.52
							–		219–246;	01.60;
							–		370–446	43.43

 $\Delta H_{\text{f corr}} = \Delta H_{\text{obs}}/\% \text{ drug in sample} \times 100$ ^a ΔT ranges between T_{onset} and T_{endset}

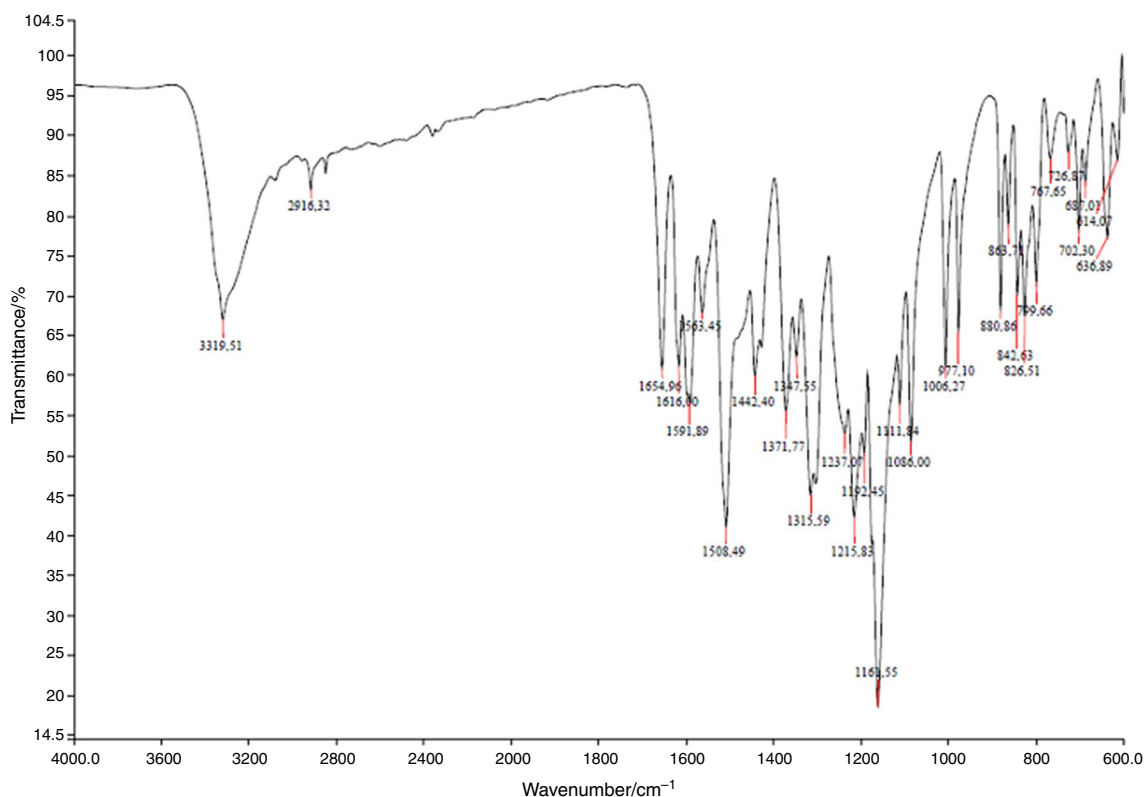


Fig. 4 FTIR spectrum of pure KPF

Table 3 Values of the bands obtained by FTIR of KPF and the mixtures carried out

Sample	Characteristic FTIR bands/cm ⁻¹					
	O–H	C=O	C=C aromatic	Vibrations of the benzene ring	C–OH	C–O
KPF	3319.51	1654.96	1616.00	1508.45	1371.77	1161.55
KPF + STR	3319.40	1655.64	1615.47	1509.59	1372.52	1163.50
KPF + MCC	3319.92	1655.91	1616.03	1509.83	1372.95	1164.01
KPF + MS	3318.02	1655.64	1616.00	1509.81	1373.79	1164.05
KPF + HPMC	3319.58	1655.57	1616.07	1509.71	1372.87	1163.88
KPF + LAC	3319.49	1655.73	1616.17	1508.89	1373.76	1164.28
KPF + SLS	3319.89	1655.68	1615.70	1509.45	1372.84	1163.48
KPF + PVP	3320.19	1654.89	1616.10	1509.76	1373.32	1164.19

band at 1371 cm⁻¹ attributed to the C=OH bond and (6) a strong band at 1161 cm⁻¹ attributed to the stretching vibration of C–O [20, 28]. The spectra of the KPF–excipient mixtures showed that the characteristic KPF bands were

practically unchanged (Table 3), indicating that the chemical structure of KPF remained unchanged (Fig. 5).

Although FTIR was an important complementary technique to DSC and TG, compatibilities were not able to be

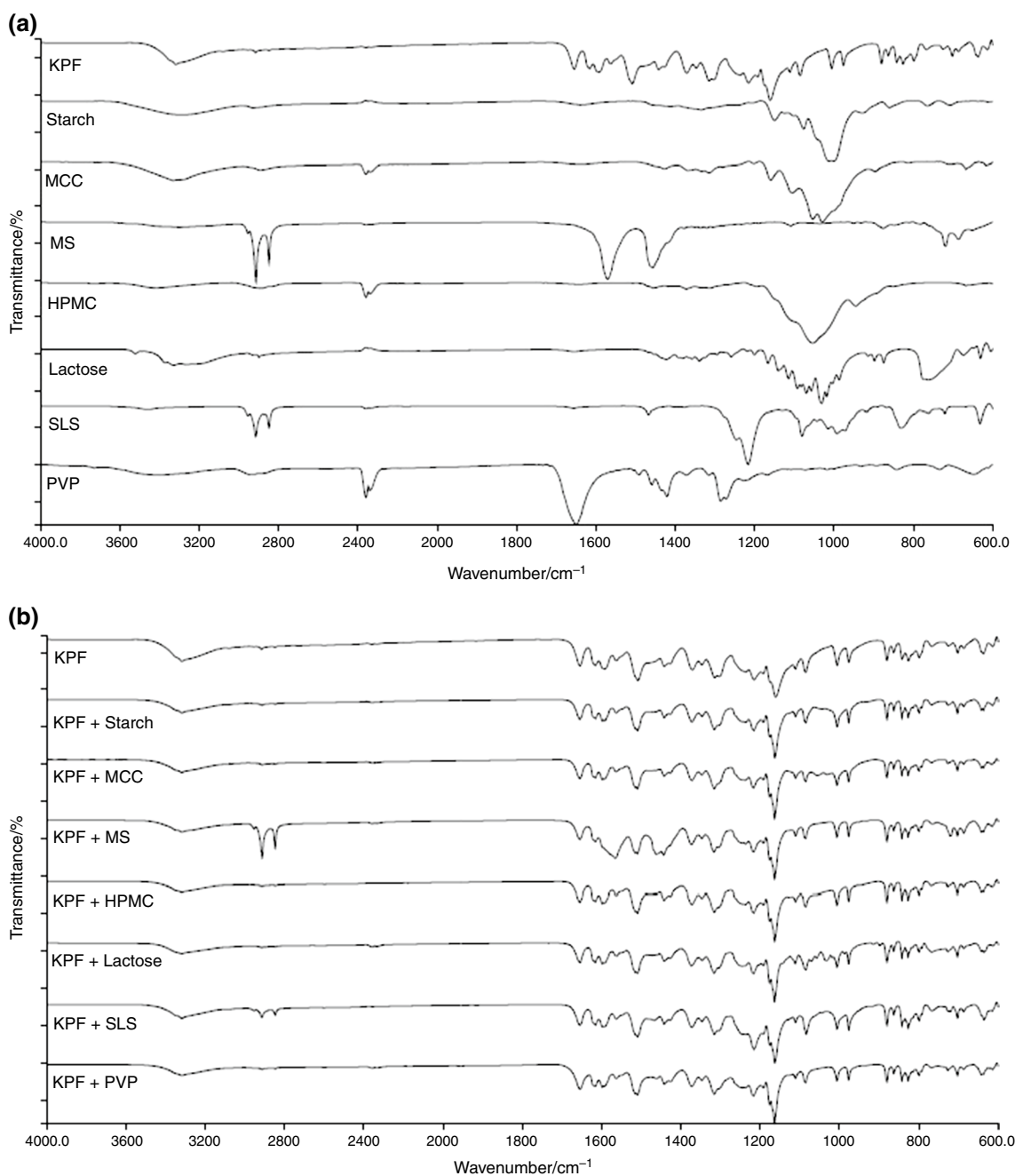


Fig. 5 Overlapping FTIR spectra of **a** KPF and excipients; **b** KPF and binary mixtures

fully confirmed by FTIR as the overlap of bands that was observed for the mixtures impaired data interpretation. Therefore, statistical techniques were required to facilitate interpretation of the spectra [7].

Multivariate statistics

Two spectral regions (3600–2800 cm⁻¹ and 1800–600 cm⁻¹) were selected for chemometric calculations. The fingerprint region of 1800–600 cm⁻¹ was

considered to be the most informative, because this region does not contain major absorption bands of the excipients and can therefore be used to identify structural changes of KPF. The 3600–2800 cm⁻¹ region is complementary to the fingerprint region as it indicates the presence of O–H, C–H and N–H groups in the molecule. In the case of the carbohydrate excipients (starch, microcrystalline cellulose and lactose), band characteristics of the stretching deformations of O–H and C–H groups were observed in this region [19].

Table 4 Results of PCA calculations for the physical mixtures of kaempferol and excipients

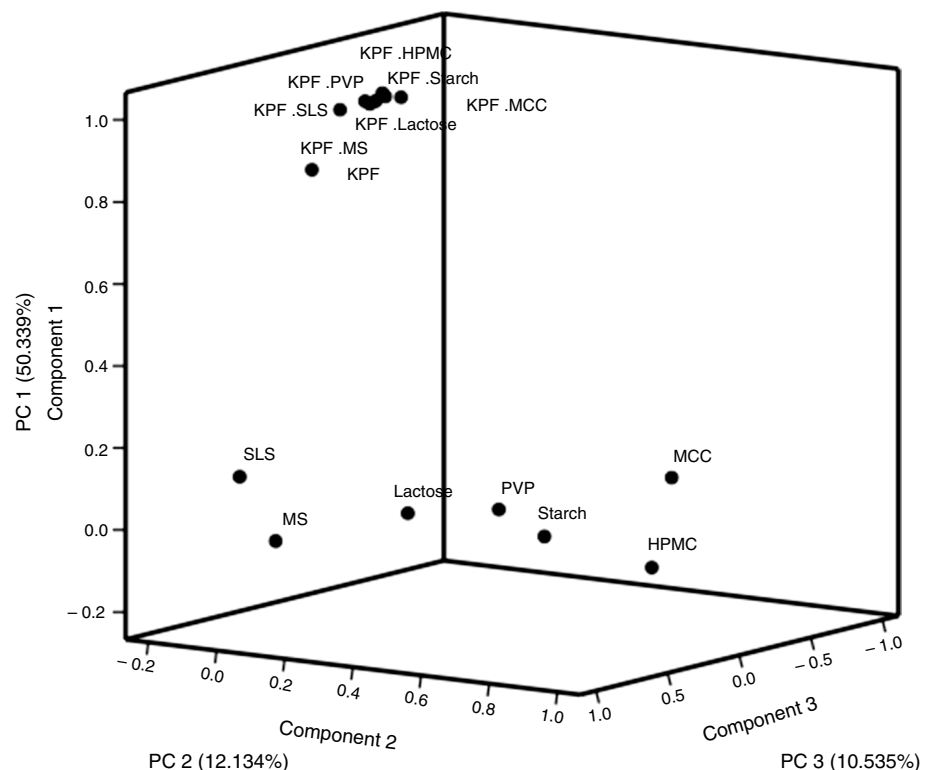
Principal component	Eigenvalue	Variance/%	Variance/% (cumulative variance/%)
1	7.551	50.339	50.339
2	1.821	12.143	62.483
3	1.580	10.535	73.018
4	1.061	7.073	80.090
5	0.999	6.600	86.690
6	0.922	6.148	92.838

Drug-excipient compatibility can be assessed from the graphical representation of the PCA, based on the distribution of analyzed samples in the bi- or three-dimensional plane [12]. In this case, the eigenvalues and variances were explained by three main components (PC1, PC2 and PC3) for the mixtures studied (Table 4). Using these components in the model retains a significant part of the variability, thus, a three-dimensional scatter diagram was appropriate to view the PCA results. Two distinct clusters, one of the excipients and one relating to the mixtures of KPF with every excipient and KPF alone, were observed (Fig. 6). The data relating

to KPF and the mixtures were located in the most positive region of PC1. Excipients were distributed more broadly, including at the most negative values of PC1, between positive and negative values of PC2 and at positive values of PC3.

The formation of two separate clusters indicates that interactions did occur within the mixtures. This separation profile occurs because the main functional groups of KPF persist in the mixture, but are located closer to the structure of KPF than to those of the excipients. Positive interactions occur between the substances but do not annul the structural properties of each. From these data, we can conclude that the substances of the mixtures were compatible.

The HCA analysis was performed to complement PCA analysis. This technique groups samples into classes based on FTIR transmittance values at certain wave numbers [12]. Results are presented as distance coefficients in the form of a dendrogram, and compatibility between ingredients is indicated when two clusters are formed [16]. The Euclidean distance (a measure of dissimilarity) was used to calculate the distance coefficients [28]. The dendrogram for KPF and the mixtures (Fig. 7) shows two large clusters, one representing KPF and the mixtures and one representing the excipients,

Fig. 6 Scatterplot of PCA in three dimensions. KPF and KPF–excipient mixtures and excipients

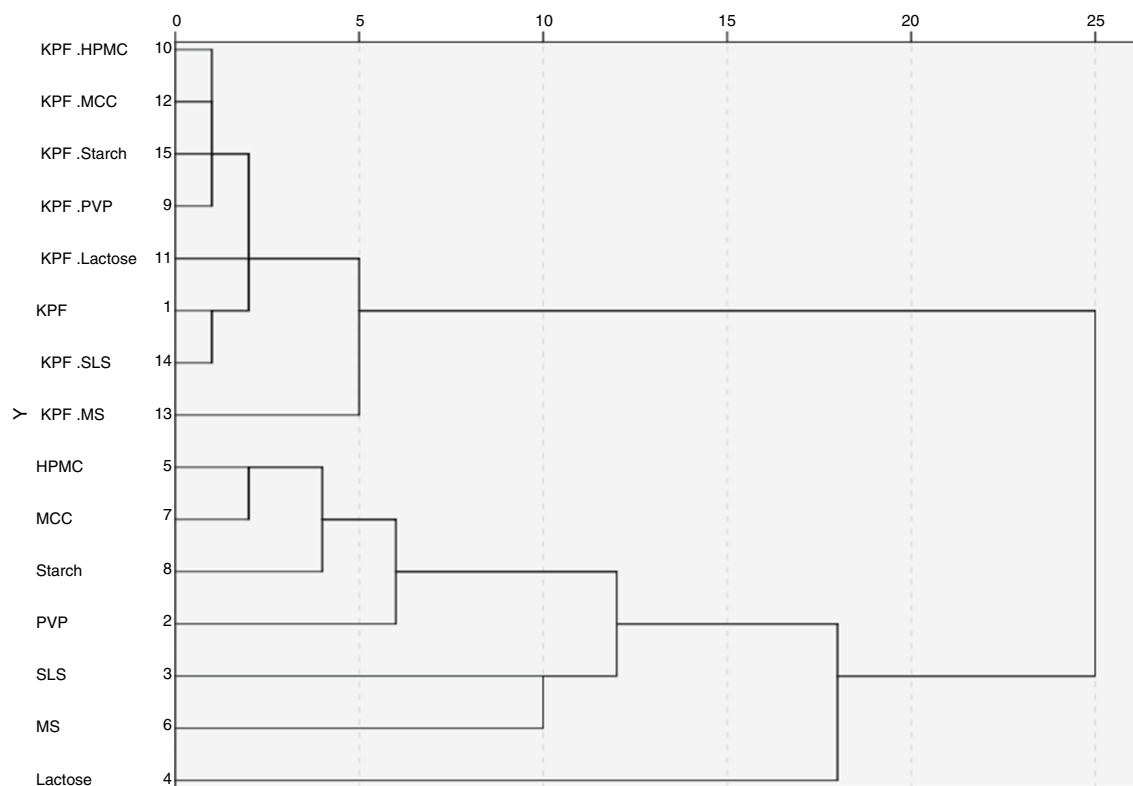


Fig. 7 Dendrogram of HCA in three dimensions showing KPF, KPF–exciipient mixtures and excipients

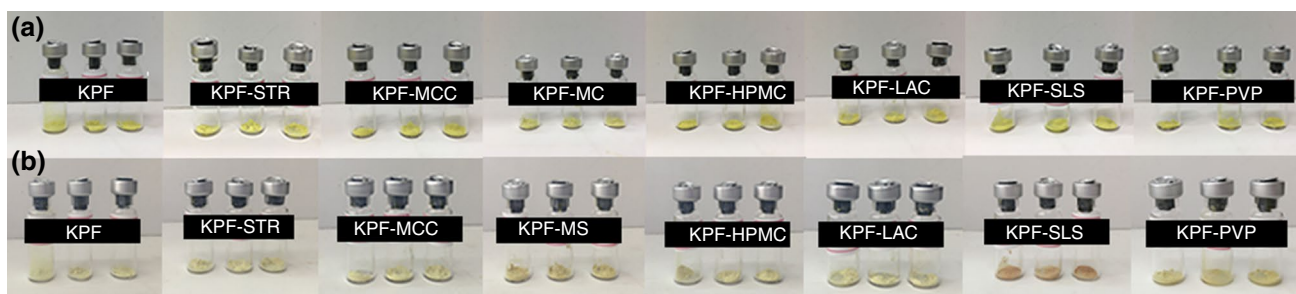


Fig. 8 Results of qualitatively analysis to identify color changes of KPF and KPF–exciipient mixtures before and after 3 weeks of storage. **a** Samples analyzes immediately after preparation. **b** Samples after 3 weeks of storage at 50 °C

thus supporting the PCA data and indicating compatibility between the constituents of mixtures.

Isothermal stress testing analysis

After three weeks of storage at 50 or 4 °C, the KPF–exciipient mixtures were qualitatively analyzed to identify color changes, and assessed by HPLC to verify the KPF content. All of the mixtures as well as KPF alone showed a small decrease in the intensity of the yellow color except

KPF–SLS which showed darkening toward a strong yellow (Fig. 8). These changes should suggest that there is interaction between the components of the blend. The retention times and peak shapes observed by quantitative HPLC (Fig. 9) indicated that there were no significant changes in the KPF content of any mixture after being submitted to the analysis conditions (Fig. 10) and the PDA peak purity revealed that the purity of all samples was > 0.999.

The results of thermal, spectroscopic and chemometric analyses are collated in Table 5. Apart from the thermal

Fig. 9 Results of the retention times and peak shapes observed by quantitative HPLC of KPF and KPF–excipient mixtures after 3 weeks of storage at 50 °C

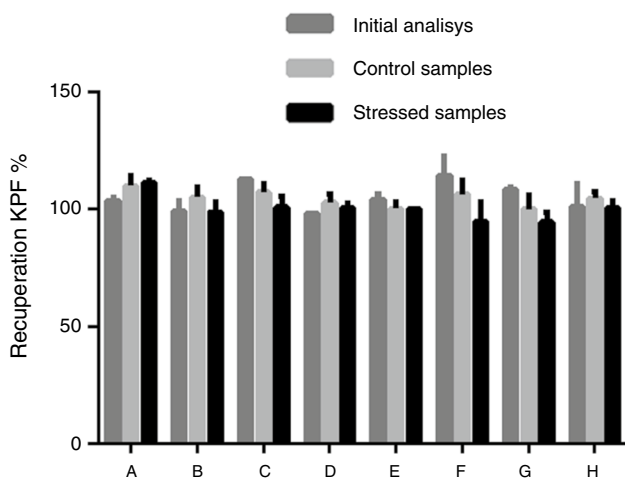
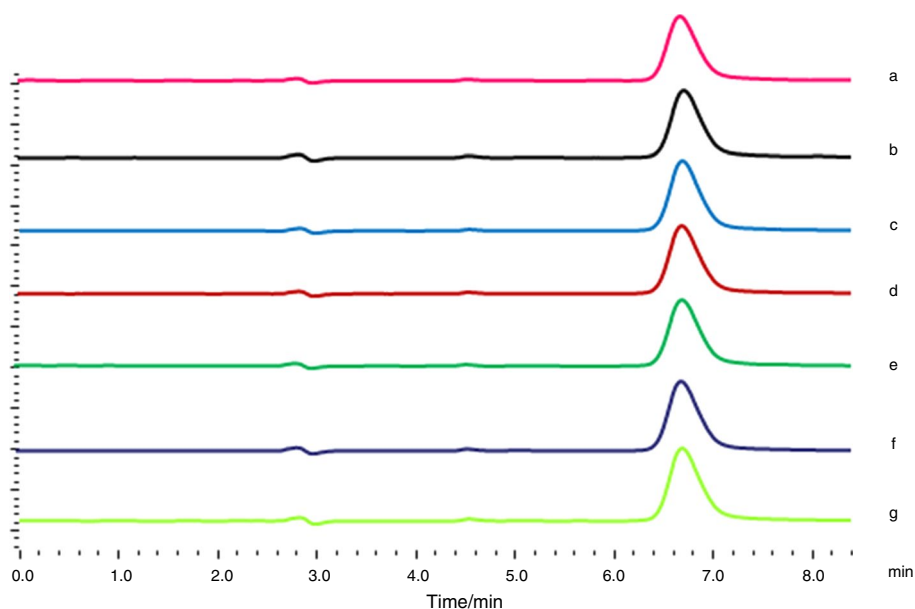


Fig. 10 Results of HPLC analysis of the KPF and KPF–excipient mixtures after 3 weeks of storage. Initial analysis: KPF–excipient mixtures analyzed immediately after preparation. Control samples: KPF–excipient mixtures without added water and stored at 4 °C for 3 weeks. Stressed samples: KPF–excipient mixtures with 10% added water and stored at 50 °C for 3 weeks. Values expressed as average \pm standard deviation. (a KPF; b KPF–STR; c KPF–MCC; d KPF–MS; e KPF–HPMC; f KPF–LAC; g KPF–SLS; h KPF–PVP)

techniques, all methods indicate compatibility between KPF and each of the excipients compatibility. However, results of DSC and TG should not be dismissed as they can still provide useful information, indicating that physicochemical interactions may have occurred between them during sample heating.

Conclusions

The present work aimed to evaluate, yet unexplored, incompatibilities between KPF and some of the most used excipients in solid dosage forms (starch, microcrystalline cellulose, magnesium stearate, hydroxypropylmethylcellulose, lactose, sodium lauryl sulfate and polyvinylpyrrolidone) using thermal statistical analysis methods, spectroscopic and multivariate analysis. Thermal analysis suggested that interactions were occurring between KPF and the excipients analyzed, except for microcrystalline cellulose. However, based on the results of FTIR and the data obtained from PCA, HCA and IST analysis, the possibility of KPF–excipient incompatibility was excluded. The statistical methods of

Table 5 Interactions between kaempferol and excipients based on thermal, FTIR spectroscopic and multivariate analysis data. The ingredients of mixtures are compatible (+) or incompatible (–)

Excipients	TG	DSC	FTIR	HCA	PCA	IST
STR	–	–	+	+	+	+
MCC	+	+	+	+	+	+
MS	–	–	+	+	+	+
HPMC	–	–	+	+	+	+
LAC	–	–	+	+	+	+
SLS	–	–	+	+	+	+
PVP	–	–	+	+	+	+

PCA and HCA were valuable tools in the interpretation of FTIR spectra. Our study highlights the importance of using multiple techniques in pre-formulation studies.

Acknowledgements This study was financed in part by Coordenação de Aperfeiçoamento de Pessoal de Nível Superior—Brasil (CAPES)—Finance Code 001 and by Fundação de Amparo à Pesquisa do Rio Grande do Sul—FAPERGS (Edital PqG 2017—Grant 17/2551-0001043-4).

References

- Pani N, Nath L, Acharya S. Compatibility studies of nateglinide with excipients in immediate release tablets. *Acta Pharmaceutica*. 2011;61:237–47.
- Wang Y, Luo YH, Zhao J, Sun BW. Selection of excipients for dispersible tablets of itraconazole through the application of thermal techniques and Raman spectroscopy. *J Therm Anal Calorim*. 2014;115:2391–400.
- Pereira MAV, Fonseca GD, Barbosa EG, Gomes APB. Compatibility study between chitosan and pharmaceutical excipients used in solid dosage forms. *J Therm Anal Calorim*. 2014;116:1091–100.
- Matos APS, Costa JS, Boniatti J, Seiceira RC, Pitaluga A, Oliveira DL, et al. Compatibility study between diazepam and tablet excipients: infrared spectroscopy and thermal analysis in accelerated stability conditions. *J Therm Anal Calorim*. 2017;127:1675–82.
- Chadha R, Bhandari S. Drug—excipient compatibility screening—Role of thermoanalytical and spectroscopic techniques. *J Pharm Biomed Anal*. 2014;87:82–97. <https://doi.org/10.1016/j.jpba.2013.06.016>.
- Fulias A, Bandur G, Marian E, Tit D. Compatibility study between ketoprofen and pharmaceutical excipients used in solid dosage forms Bogdan Tit. *J Pharm Biomed Anal*. 2011;56:221–7.
- Rojek B, Wesolowski M. Fourier transform infrared spectroscopy supported by multivariate statistics in compatibility study of atenolol with excipients. *Vib Spectrosc*. 2016;86:190–7.
- Monajjemzadeh F, Hassanzadeh D, Valizadeh H, Siah-shadbad MR, Shahbazi J, Robertson TA, et al. Compatibility studies of acyclovir and lactose in physical mixtures and commercial tablets. *Eur J Pharm Biopharm*. 2009;73:404–13. <https://doi.org/10.1016/j.ejpb.2009.06.012>.
- Rajalahti T, Kvalheim OM. Multivariate data analysis in pharmaceuticals: A tutorial review. *Int J Pharm*. 2011;417:280–90. <https://doi.org/10.1016/j.ijpharm.2011.02.019>.
- Wesolowski M, Rojek B. Thermogravimetric detection of incompatibilities between atenolol and excipients using multivariate techniques. *J Therm Anal Calorim*. 2013;113:169–77.
- Souza J, Daniel P, Pianna I, Lopes L, Trevisan MG, Simone J. Risperidone—solid-state characterization and pharmaceutical compatibility using thermal and non-thermal techniques. *Thermochim Acta*. 2013;568:148–55.
- Rojek B, Wesolowski M, Suchacz B. Spectrochimica acta part a : molecular and biomolecular spectroscopy detection of compatibility between baclofen and excipients with aid of infrared spectroscopy and chemometry. *Spectrochim Acta Part A Mol Biomol Spectrosc*. 2013;116:532–8. <https://doi.org/10.1016/j.saa.2013.07.102>.
- Wesolowski M, Rojek B, Piotrowska J. Application of chemometrically processed thermogravimetric data for identification of baclofen-exciptent interactions. *J AOAC Int*. 2012;95:691–8.
- Rojek B, Wesolowski M. Compatibility studies of hydrocortisone with excipients using thermogravimetric analysis supported by multivariate statistical analysis. *J Therm Anal Calorim*. 2017;127:543–53.
- Wang SY, Chen C, Wang CY. The influence of light and maturity on fruit quality and flavonoid content of red raspberries. *Food Chem*. 2009;112:676–84.
- Zhang K, Gu L, Chen J, Zhang Y, Jiang Y, Zhao L, et al. Preparation and evaluation of kaempferol – phospholipid complex for pharmacokinetics and bioavailability in SD rats. *J Pharm Biomed Anal*. 2015;114:168–75. <https://doi.org/10.1016/j.jpba.2015.05.017>.
- Devi KP, Malar DS, Nabavi SF, Sureda A, Xiao J, Nabavi SM, et al. Kaempferol and inflammation: from chemistry to medicine. *Pharmacol Res*. 2015;99:1–10. <https://doi.org/10.1016/j.phrs.2015.05.002>.
- Kim S, Choi K. Anti-cancer effect and underlying mechanism (s) of kaempferol, a phytoestrogen, on the regulation of apoptosis in diverse cancer cell models. *Toxicol Res*. 2013;29:229–34.
- Chen ZP, Sun J, Chen HX, Xiao YY, Liu D, Chen J, et al. Comparative pharmacokinetics and bioavailability studies of quercetin, kaempferol and isorhamnetin after oral administration of Ginkgo biloba extracts, Ginkgo biloba extract phospholipid complexes and Ginkgo biloba extract solid dispersions in rats. *Fitoterapia*. 2010;81:1045–52. <https://doi.org/10.1016/j.fitote.2010.06.028>.
- Li W, Yi S, Wang Z, Chen S, Xin S, Xie J, et al. Self-nanoemulsifying drug delivery system of persimmon leaf extract : Optimization and bioavailability studies. *Int J Pharm*. 2011;420:161–71. <https://doi.org/10.1016/j.ijpharm.2011.08.024>.
- Calderon-Montano JM, Burgos-Moron E, Perez-Guerrero C, Lopez-Lazaro M. A Review on the Dietary Flavonoid Kaempferol. *Mini Rev Med Chem*. 2011;11(47):298–344.
- Barvea A, Chenc C, Hebbbar V, Desiderioa J. Constance lay-lay Sawb and A-NK. metabolism, oral bioavailability and pharmacokinetics of chemopreventive kaempferol in rats. *Biopharm Drug Dispos*. 2009;30:356–65.
- Cao J, Zhang Y, Chen W, Zhao X. The relationship between fasting plasma concentrations of selected flavonoids and their ordinary dietary intake. *Br J Nutr*. 2010;103:249–55.
- Trivedi R, Kumar S, Kumar A, Siddiqui JA, Swarnkar G, Gupta V, et al. Kaempferol has osteogenic effect in ovariectomized adult Sprague–Dawley rats. *Mol Cell Endocrinol*. 2008;289:85–93.
- Trivedi R, Kumar A, Gupta V, Kumar S, Nagar GK, Romero JR, et al. Effects of Egb 761 on bone mineral density, bone microstructure, and osteoblast function: possible roles of quercetin and kaempferol. *Mol Cell Endocrinol*. 2009;302:86–91.
- IBM Corp. Released 2013. IBM SPSS Statistics for Windows, Version 22.0. IBM Corp, Armonk, NY
- Colombo M, de Lima Melchiades G, Figueiró F, Battastini AMO, Teixeira HF, Koester LS. Validation of an HPLC-UV method for analysis of kaempferol-loaded nanoemulsion and its application to in vitro and in vivo tests. *J Pharm Biomed Anal*. 2017;145:831–7.
- Hayton JC, Allen DG, Scarpello V. Factor retention decisions in exploratory factor analysis: a tutorial on parallel analysis. *Org Res Methods*. 2004;7(2):191–205.

Publisher's Note Springer Nature remains neutral with regard to jurisdictional claims in published maps and institutional affiliations.